International Journal of Production Research
Vol. 50, No. 22, 15 November 2012, 6624–6638

Taylor & Francis
Taylor & Francis Group

Monitoring multivariate process variability with individual observations via penalised likelihood estimation

Arthur B. Yeh[a], Bo Li[b] and Kaibo Wang[c]*

[a]*Department of Applied Statistics and Operations Research, Bowling Green State University, Bowling Green, OH 43403, USA;* [b]*Research Center for Contemporary Management, Key Research Institute of Humanities and Social Sciences at Universities, School of Economics and Management, Tsinghua University, Beijing 100084, China;* [c]*Department of Industrial Engineering, Tsinghua University, Beijing 100084, China*

(*Received 5 October 2011; final version received 9 March 2012*)

Excessive variation in a manufacturing process is one of the major causes of a high defect rate and poor product quality. Therefore, quick detection of changes, especially increases in process variability, is essential for quality control. In modern manufacturing environments, most of the quality characteristics that have to be closely monitored are multivariate by the nature of the applications. In these multivariate settings, the monitoring of process variability is considerably more difficult than monitoring a univariate variance, especially if the manufacturing environment only allows for the collection of individual observations. Some recent charts, such as the MaxMEWMV chart, the MEWMS chart and the MEWMC chart, have been proposed to monitor process variability specifically when the subgroup size is equal to 1. However, these methods do not take into account the engineering and operational understanding of how the process works. That is, when the process variability goes out of control, it is often the case that changes only occur in a small number of elements of the covariance matrix or the precision matrix. In this work, we propose a control charting mechanism that enhances the existing methods via penalised likelihood estimation of the precision matrix when only individual observations are available for monitoring the process variability. The average run length of the proposed chart is compared with that of the MaxMEWMV, MEWMS and MEWMC charts. A real example is also presented in which the proposed chart and the existing charts are applied and compared.

Keywords: control charts; quality control; covariance matrix; penalty function; likelihood ratio test; penalised likelihood function; phase II monitoring; sparsity

1. Introduction

Excessive variation in a manufacturing process is one of the major causes of a high defect rate and poor quality of manufactured products. For example, in a wafer fabrication process, changes in variation are usually caused by changes of raw materials, deterioration of key equipment, incorrect settings of process parameters, etc. Such root causes, if not identified and removed quickly, will inevitably have a negative impact on the final product quality and, in turn, the process yield. In an example related to ambulatory monitoring, Hawkins and Maboudou-Tchao (2008) noted that it was instrument change-out that caused variance/covariance components to change. In another example related to a multistage manufacturing environment, the process variation propagated from upstream to downstream stages, and thus had to be monitored closely for unexpected changes (Shi 2006). Therefore, the quick detection of changes in process variation is essential for quality control.

In modern manufacturing environments, most of the quality characteristics that have to be closely monitored are multivariate by the nature of the applications. In these multivariate settings, the monitoring of process variability is considerably more difficult than monitoring a univariate variance. Numerous control charts for monitoring multivariate process variability have appeared in the literature to date. Apart from the different charting statistics these charts use, they also differ in the assumption of the subgroup size needed. Some methods assume that the subgroup size is larger than the dimensionality of the quality characteristic to be monitored. In this case, when a sample of observations is collected, an estimate of the process covariance matrix can be obtained and compared with an in-control value. Earlier work by, for example, Montgomery and Wadsworth (1972) and Alt (1984), falls into this category. Montgomery and Wadsworth (1972) proposed to monitor the determinant of the process covariance

*Corresponding author. Email: kbwang@tsinghua.edu.cn

ISSN 0020–7543 print/ISSN 1366–588X online

http://dx.doi.org/10.1080/00207543.2012.676684
http://www.tandfonline.com

matrix, commonly referred to as the generalised variance, via the determinant of the sample covariance matrix, while Alt (1984) proposed to monitor the generalised likelihood ratio (GLR) for testing the hypothesis that the process covariance matrix is equal to a pre-specified value. Since the information collected in each sampling period is assumed to be sufficient for estimating the covariance matrix, these methods are usually Shewhart-type control charts that do not take into account historical observations.

In many industrial applications, the practical subgroup size is either small or even equal to one such that the process covariance matrix cannot be estimated based on each sample alone. In these cases, it is therefore imperative that historical observations be accumulated in a certain way in order to more effectively estimate the process covariance matrix. The maximum multivariate exponentially weighted moving variability (MaxMEWMV) chart of Yeh *et al*. (2005), the multivariate exponentially weighted mean squared deviation (MEWMS) chart and the multivariate exponentially weighted variance (MEWMV) chart of Huwang *et al*. (2007), and the multivariate exponentially weighted moving covariance (MEWMC) chart of Hawkins and Maboudou-Tchao (2008), all accumulate historical observations by taking the EWMA of some statistics developed based on individual observations (i.e. the subgroups size is one). In these multivariate EWMA charts, the EWMA smoothing of historical observations provides a practical way to improve the estimation accuracy given the limited amount of information available at each sampling period. It should be noted that Zhang and Chang (2008) proposed a multivariate exponentially weighted moving deviation (MEWMD) chart for monitoring only the variance components for individual observations. The MEWMD chart is essentially an extension of the multivariate exponentially weighted moving average (MEWMA) chart of Lowry *et al*. (1992) and it is not intended to detect changes in the covariance components.

The existing control charts for monitoring process variability, Shewhart- or EWMA-type, share one common feature, that is they all rely on the sample covariance matrix or its EWMA version for estimating the process covariance matrix. Such an approach, given that data are inevitably contaminated by noise, does not take into account any knowledge of the process covariance matrix stemming from an engineering and operational understanding of how the process works. For a simple illustration of the point just raised, let us assume that the in-control process covariance matrix is an identity matrix, which is a common assumption of Phase˜II control charts for monitoring the process covariance matrix. Nevertheless, under such an assumption, the sample covariance matrix or its EWMA version is likely to contain mostly non-zero off-diagonal elements even if the process covariance remains in control. Further, in many practical applications, when process variability changes, it is often the case that such changes are seen in only a small number of elements in the covariance matrix or the precision matrix, which is the inverse of the covariance matrix. This implies that sample covariance matrix based control charts are likely to contain information not pertinent to the true process variability, which, as a result, may hamper the performance of the existing charts. More specifically, the type of process variability changes to be quickly detected in Phase II is likely to be sparse in that only few of the off-diagonal elements of the covariance or precision matrix will be non-zero. Therefore, the sparsity of the matrix should be incorporated into the design of control charts for monitoring the process variability. This consideration is the main motivation behind the current study.

A sparse estimate of a covariance matrix or precision matrix is also statistically appealing. Under observational noise, a sparse estimate is more stable (Huang *et al*. 2006). Recently, much work has appeared in the literature concerning how to obtain sparse estimates of a covariance matrix (see, e.g., Rothman *et al*. (2008), D'Aspremont *et al*. (2008) and Friedman *et al*. (2008)). In multivariate control chart applications, the precision matrix has important engineering implications. If the ith row and jth column element of the precision matrix is equal to 0, it means the ith and jth variables are conditionally independent given all other variables. In quality analysis, such conditional independence indicates that quality deterioration of one variable should not be attributed to the other variable, although the marginal correlation between these two variables may be quite significant. Such implications are important to root cause diagnosis. Therefore, the sparsity of the precision matrix can be linked with engineering knowledge and be used to improve the performance of the control charting mechanism.

Considering that the covariance structure to be monitored is likely sparse, we propose in this work a new Phase II control chart for monitoring the process variability that takes such information into account. The proposed chart is constructed by first accumulating individual observations through an EWMA calculation. A sparse estimate of the precision matrix is then obtained based on the smoothed EWMA sample matrix via penalised likelihood estimation. The estimate thus obtained is then used in a likelihood ratio test based charting static to detect changes in the covariance matrix. It should be pointed out that, in a very recent study by Li *et al*. (2012), a Shewhart-type control chart was proposed to monitor a sparse covariance matrix. However, the sample size required was much larger than the dimensionality of the quality characteristic to be monitored.

The rest of the paper is organised as follows. In Section 2, after briefly introducing the existing control charts, a detailed discussion of the proposed control chart is given. Section 3 is devoted to numerical studies comparing the chart performance of the proposed chart and the existing charts. In Section 4, the proposed chart is applied to a real example and compared with the existing methods. Concluding remarks and a discussion of potential future research along the same lines are given in Section 5.

2. The proposed control charting mechanism

2.1 *The existing control charts*

Let $\mathbf{X}$ denote the p-dimensional quality characteristic to be monitored and assume that $\mathbf{X}$ follows a p-dimensional normal distribution denoted as $N(\boldsymbol{\mu}, \boldsymbol{\Sigma})$, where $\boldsymbol{\mu}$ and $\boldsymbol{\Sigma}$ are the mean and covariance matrix of the distribution, respectively. When the process is in control, we assume that $\boldsymbol{\mu} = \boldsymbol{\mu}_0$ and $\boldsymbol{\Sigma} = \boldsymbol{\Sigma}_0$. Since our focus in the current paper is on Phase II monitoring, as is the case in most literature on Phase II control charts, we assume that $\boldsymbol{\mu}_0$ and $\boldsymbol{\Sigma}_0$ are either known or can be reasonably estimated based on the data collected from Phase I control when the process was in control. Our primary interest in the current work is developing control charts for monitoring changes in process variability and, therefore, we further assume that when the process is out of control, the process covariance matrix changes to $\boldsymbol{\Sigma}_{OC} \neq \boldsymbol{\Sigma}_0$ while the process mean remains in control and the change is sustained throughout the monitoring operation. For recent work on multivariate control charts for monitoring the process mean, see, for example, Gonzalez and Sanchez (2008), Hwarng (2008), Alfaro *et al.* (2009), Niaki and Davoodi (2009), and Hwarng and Wang (2010).

Alt (1984) proposed a Phase II control chart for monitoring $\boldsymbol{\Sigma}$ whose plotting statistic for the ith sample, $i = 1, 2, \ldots$, is the generalised likelihood ratio (GLR) for testing H_0: $\boldsymbol{\Sigma} = \boldsymbol{\Sigma}_0$:

$$W_i = -(m-1)\left[p + \ln\frac{|\mathbf{S}_i|}{|\boldsymbol{\Sigma}_0|} - \mathrm{tr}(\boldsymbol{\Sigma}_0^{-1}\mathbf{S}_i)\right], \tag{1}$$

where $|A|$ is the determinant of the matrix A, $\mathrm{tr}(B)$ is the trace of the matrix B, m is the subgroup size, p is the process dimension, and $\mathbf{S}_i$ is the sample covariance matrix calculated based on the ith sample.

As discussed above, the type of Shewhart chart for monitoring $\boldsymbol{\Sigma}$ which relies on $\mathbf{S}_i$ typically assumes that $m > p$. However, in the case when $m = 1$, $\mathbf{S}_i$ based Shewhart charts are not applicable. Huwang *et al.* (2007) and Hawkins and Maboudou-Tchao (2008) both proposed to first transform the individual observation, $\mathbf{X}_i$, into $\mathbf{U}_i = \boldsymbol{\Sigma}_0^{-1/2}(\mathbf{X}_i - \boldsymbol{\mu}_0)$, such that when the process is in control, $\mathbf{U}_i$ is distributed as $N(\mathbf{0}, \mathbf{I}_p)$, where $\mathbf{I}_p$ is a $p \times p$ identity matrix. The individual $\mathbf{U}_i$ values are then accumulated based on an EWMA calculation:

$$\mathbf{S}_i = (1-\omega)\mathbf{S}_{i-1} + \omega\mathbf{U}_i\mathbf{U}_i^T, \tag{2}$$

where $\mathbf{S}_0 = \mathbf{I}_p$ and $0 < \omega < 1$ is a smoothing constant. To simplify notation, here we continue to use $\mathbf{S}_i$ to denote the estimate of the covariance matrix based on the EWMA calculation.

Huwang *et al.* (2007) use $\mathrm{tr}(\mathbf{S}_i)$ as the plotting statistic of the MEWMS chart. Hawkins and Maboudou-Tchao (2008) plug $\mathbf{S}_i$ into the GLR calculation in Equation (1) to form the charting statistic of the MEWMC chart:

$$c_i = \mathrm{tr}(\mathbf{S}_i) - \log|\mathbf{S}_i| - p. \tag{3}$$

For the MaxMEWMV chart of Yeh *et al.* (2005), the plotting statistic is equal to (for $i = 1, 2, \ldots$)

$$\max D_i = \max\left[\frac{D_{i1} - E(D_{i1})}{\sqrt{\mathrm{Var}(D_{i1})}}, \frac{D_{i2} - E(D_{i2})}{\sqrt{\mathrm{Var}(D_{i2})}}\right], \tag{4}$$

where $D_{i1} = \sqrt{\sum_{j=1}^{p}(s_i(jj)-1)^2}$, $D_{i2} = \sqrt{\sum_{j=1}^{p}\sum_{1\le k<j\le p} s_i^2(jk)}$ and $\mathbf{S}_i = [s_i(jk)]_{p\times p}$. D_{i1} is essentially the Euclidean distance between the vector of p diagonal elements of $\mathbf{S}_i$ and its in-control value, which is a vector of 1's. Similarly, D_{i2} is the Euclidean distance between the vector of $p(p-1)/2$ lower triangular off-diagonal elements of $\mathbf{S}_i$ and its in-control value, which is a vector of 0's. Therefore, the changes in the covariance matrix can be reflected in either or both of the deviations of the variance and covariance components from their in-control values.

2.2 *The LASSO-MEWMC chart*

Although the EWMA accumulation of historical observations in Equation (2) is expected to result in a more stable estimate of the process covariance matrix when only individual observations are available, the resulting $\mathbf{S}_i$ does not take into account any knowledge of the structure of the covariance matrix. For example, when the process is in control, the expected value of $\mathbf{S}_i$ is equal to $\mathbf{I}_p$, the structure of which is basically sparse. However, the estimate $\mathbf{S}_i$ will likely contain mostly non-zero off-diagonal elements. Therefore, in this work, we propose to obtain a sparse estimate of the precision matrix based on $\mathbf{S}_i$, and use this estimate to construct the proposed control charting mechanism. Define $\mathbf{\Omega}_0 = \mathbf{\Sigma}_0^{-1}$, which is the in-control precision matrix of a process whose in-control covariance matrix is equal to $\mathbf{\Sigma}_0$. Since we are dealing with $\mathbf{U}_i$, the transformed variables, in the EWMA context, $\mathbf{\Omega}_0 = \mathbf{\Sigma}_0^{-1} = \mathbf{I}_p^{-1} = \mathbf{I}_p$. Following Equation (2), we define $\hat{\mathbf{\Omega}}_\lambda$ as the solution to the following penalised likelihood function:

$$\hat{\mathbf{\Omega}}_\lambda = \arg\min_{\Omega>0}\{\mathrm{tr}(\mathbf{\Omega}\mathbf{S}_i) - \ln|\mathbf{\Omega}| + \lambda\|\mathbf{\Omega} - \mathbf{I}_p\|_1\}, \tag{5}$$

where $\|\mathbf{A}\|_1 = \sum_{j=1}^{p}\sum_{i=1}^{p}|a_{ij}|$ for $\mathbf{A} = [a_{ij}]_{p\times p}$, and λ is a data-dependent tuning parameter that can be tuned to achieve different levels of sparsity of the resulting $\hat{\mathbf{\Omega}}_\lambda$.

The added penalty term in Equation (5) is helpful in forming the desired structure in the precision matrix. Similar penalty functions have been studied in the literature. Rothman *et al.* (2008) considered a different penalty term, $\lambda\|\mathbf{\Omega} - \mathrm{diag}(\mathbf{\Omega})\|_1$, which penalises all off-diagonal but ignores diagonal elements of $\mathbf{\Omega}$. D'Aspremont *et al.* (2008) and Friedman *et al.* (2008) investigated the use of the penalty $\lambda\|\mathbf{\Omega}\|_1$, which penalises all elements of $\mathbf{\Omega}$. This has the effect of forcing all elements, including diagonal elements, to zero. However, in control chart applications, all elements should be forced to shrink towards their respective in-control values. If all process variables are transformed such that $\mathbf{\Sigma}_0 = \mathbf{I}_p$, the in-control values of the off-diagonal elements should all be zero and the in-control values of the diagonal elements should all be one. Therefore, if used directly in control chart applications, i.e. penalising the elements in $\mathbf{\Omega}$, Rothman *et al.*'s (2008) penalty ignores noise in variance terms, while the penalty used by D'Aspremont *et al.* (2008) and Friedman *et al.* (2008) inappropriately forces variance components to zero rather than one. Instead, the penalty we propose in Equation (5) penalises the distance between the diagonal elements and one, and the distance between off-diagonal elements and zero. Such an approach is designed to shrink all elements towards their respective in-control values. Therefore, Equation (5) is a more suitable choice than other forms of penalty function.

In order to detect changes in the covariance matrix, we consider the GLR for testing H_0: $\mathbf{\Sigma} = \mathbf{I}_p$ vs. H_1: $\mathbf{\Sigma} \neq \mathbf{I}_p$. With the sample covariance matrix that appears in the likelihood function being replaced by $\mathbf{S}_i$ in Equation (2), the negative log-likelihood function under H_0 is equal to, up to a constant,

$$l_0 = \mathrm{tr}(\mathbf{S}_i), \tag{6}$$

and the negative log-likelihood under H_1 is equal to, up to a constant,

$$l_1 = \mathrm{tr}(\hat{\mathbf{\Omega}}\mathbf{S}_i) - \ln|\hat{\mathbf{\Omega}}|, \tag{7}$$

where $\hat{\mathbf{\Omega}}$ is the maximum likelihood estimate (m.l.e.) of $\mathbf{\Sigma}_0^{-1}$.

Conventionally, $\hat{\mathbf{\Omega}}$ is replaced by the inverse of the sample covariance matrix, $\mathbf{S}^{-1}$. In this work, we use the sparse estimate, $\hat{\mathbf{\Omega}}_\lambda$, obtained from Equation (5) instead. Finally, the negative log-likelihood ratio becomes

$$\Lambda_\lambda = \ln|\hat{\mathbf{\Omega}}_\lambda| - \mathrm{tr}(\hat{\mathbf{\Omega}}_\lambda\mathbf{S}_i) + \mathrm{tr}(\mathbf{S}_i). \tag{8}$$

The above statistic becomes the smallest under the null hypothesis and increases otherwise; its value also varies with λ. Therefore, our proposed Phase II control chart is based on calculating the test statistic in (8) for each of the ith samples, $i = 1, 2, \ldots$. At each step, when a new observation arrives, it is first transformed into $\mathbf{U}_i$. $\mathbf{S}_i$ is updated based on Equation (2). The updated matrix is then plugged into Equation (5) to obtain a sparse estimate $\hat{\mathbf{\Omega}}_\lambda$. Finally, based on Equation (8), $\mathbf{S}_i$ and $\hat{\mathbf{\Omega}}_\lambda$ are used to calculate the charting statistic Λ_λ. The chart signals if Λ_λ exceeds a predetermined control limit, UCL_λ. The choice of UCL_λ depends on the desirable in-control performance, the dimensionality as well as on the tuning parameter λ. Listed in Table 1 are different values of UCL_λ, which were obtained based on Monte-Carlo simulation, for various tuning parameters and dimensionalities, and when the in-control average run length (ARL) is set at 200, 370 and 500.

Since this chart is derived from a sparse estimate of $\mathbf{\Omega}$ based on a least absolute shrinkage and selection operator (lasso) type penalty, we call this chart a Lasso-MEWMC (LMEWMC) chart. From the work of Yeh *et al.* (2005),

Table 1. Values of UCL_λ for different values of λ, p and in-control ARL ($\omega = 0.1$).

	$ARL_0 = 200$			$ARL_0 = 370$			$ARL_0 = 500$		
λ	$p = 5$	$p = 10$	$p = 20$	$p = 5$	$p = 10$	$p = 20$	$p = 5$	$p = 10$	$p = 20$
0.02	1.5367	4.2166	13.2953	1.6713	4.4188	13.6354	1.7334	4.5129	13.7859
0.04	1.5021	4.0267	12.2063	1.6367	4.2273	12.5398	1.6981	4.3220	12.6883
0.06	1.4617	3.8369	11.3082	1.5964	4.0398	11.6410	1.6577	4.1333	11.7875
0.08	1.4203	3.6592	10.5438	1.5555	3.8582	10.8752	1.6154	3.9528	11.0219
0.1	1.3789	3.4887	9.8672	1.5145	3.6930	10.2047	1.5758	3.7863	10.3500
0.2	1.1820	2.7762	7.3266	1.3234	2.9887	7.6727	1.3869	3.0871	7.8271
0.3	1.0039	2.2048	5.4736	1.1488	2.4172	5.8273	1.2163	2.5207	5.9906
0.4	0.8371	1.7143	3.9766	0.9849	1.9238	4.3281	1.0527	2.0281	4.4845
0.8	0.3836	0.6309	1.0846	0.5104	0.7882	1.2883	0.5696	0.8660	1.3894
1.0	0.2396	0.4107	0.6484	0.3681	0.5434	0.8137	0.4269	0.6094	0.8946
1.2	0.0625	0.2406	0.4151	0.2202	0.3808	0.5594	0.2869	0.4443	0.6276

Huwang *et al*. (2007) and Hawkins and Maboudou-Tchao (2008), it is clear that when estimating process variability based on individual observations, using EWMA to smooth the sample covariance matrix calculated from each individual observation is an effective choice against process noise. The EWMA smoothing also has the effect of accumulating historical information for a more stable estimate. In this work, we propose to obtain a sparse estimate of the precision matrix on the basis of the smoothed EWMA of $\mathbf{S}_i$. Based on the special structural information stemming from an understanding of how the process works, we propose to penalise both off-diagonal and diagonal elements of the matrix that is formed by taking the difference of the estimated and in-control precision matrices. Such a treatment is expected to help improve the chart performance. In the following section, we compare the performance of the proposed LMEWMC chart with that of the MEWMC and other charts discussed earlier for monitoring the process covariance matrix.

3. Performance study and design guidelines

3.1 *Performance of the lasso penalty*

As discussed above, the penalty proposed in Equation (5) has the effect of shrinking all elements of the estimated precision matrix towards their respective in-control values, which, under the assumption, are zero for the off-diagonal and one for the diagonal elements. Friedman *et al*. (2008) introduced an algorithm that uses the L_1 penalty of the absolute value of all elements in the precision matrix and provided an open-source package called GLasso. The GLasso algorithm can also be configured to penalise only the off-diagonal elements of the precision matrix. The algorithmic implementation of the proposed penalty in Equation (5) is a modification of the GLasso package.

We first demonstrate and compare the effects of various penalty functions on the estimation of sparse covariance and precision matrices. A random sample of 10 observations was first generated from $\mathbf{I}_p$ with $p = 5$. Although the LMEWMC chart uses an EWMA to accumulate historical observations, for demonstration, here we simply calculate the sample covariance matrix of these 10 observations. The sample covariance matrix is then put into Equation (5) to obtain a sparse estimate of the precision matrix. Finally, a sparse estimate of the covariance matrix is obtained by calculating the inverse of the estimated sparse precision matrix. Different types of penalty functions were tested and the resulting estimates are shown in Table 2, along with the corresponding un-penalised sample covariance matrix and sample precision matrix. All diagonal elements in the covariance matrix estimate and the precision matrix estimate are highlighted for clarity. It is evident from Table 2 that the sample covariance and precision matrices fail to produce the sparse structure as seen in the true covariance and precision matrices.

If Friedman *et al*.'s (2008) algorithm is applied to penalise all elements, most of the off-diagonal elements in the estimated precision matrix are shrunk to zero, while some of the diagonal elements also become smaller and are shrunk towards zero. Further, if Friedman *et al*.'s (2008) algorithm is applied to penalise only the off-diagonal elements, most of the off-diagonal elements of the estimated precision matrix are shrunk to zero, while some of the diagonal elements are also affected and shrunk towards zero. On the other hand, the penalty proposed in Equation (5) in the current paper tends to shrink all diagonal elements closer to one and at the same time off-diagonal elements towards zero. This simple example indicates that the proposed penalty in Equation (5), which is slightly

Table 2. Comparison of different types of penalties ($\lambda = 0.2$).

	Covariance matrix					Precision matrix				
	1	2	3	4	5	1	2	3	4	5
Sample										
1	**1.460**	0.119	0.652	−0.169	0.140	**0.875**	−0.067	−0.371	0.096	−0.080
2	0.119	**0.821**	0.117	−0.030	0.025	−0.067	**1.238**	−0.067	0.017	−0.014
3	0.652	0.117	**1.444**	−0.167	0.138	−0.371	−0.067	**0.884**	0.095	−0.079
4	−0.169	−0.030	−0.167	**0.843**	−0.036	0.096	0.017	0.095	**1.225**	0.020
5	0.140	0.025	0.138	−0.036	**0.830**	−0.080	−0.014	−0.079	0.020	**1.233**
Proposed penalty										
1	**1.260**	0	0.452	0	0	**0.913**	0	−0.332	0	0
2	0	**1**	0	0	0	0	**1**	0	0	0
3	0.452	0	**1.244**	0	0	−0.332	0	**0.924**	0	0
4	0	0	0	**1**	0	0	0	0	**1**	0
5	0	0	0	0	**1**	0	0	0	0	**1**
Penalising all elements										
1	**1.660**	0	0.452	0	0	**0.651**	0	−0.179	0	0
2	0	**1.021**	0	0	0	0	**0.979**	0	0	0
3	0.452	0	**1.644**	0	0	−0.179	0	**0.657**	0	0
4	0	0	0	**1.043**	0	0	0	0	**0.959**	0
5	0	0	0	0	**1.030**	0	0	0	0	**0.971**
Penalising only off-diagonal elements										
1	**1.460**	0	0.452	0	0	**0.758**	0	−0.237	0	0
2	0	**0.821**	0	0	0	0	**1.218**	0	0	0
3	0.452	0	**1.444**	0	0	−0.237	0	**0.767**	0	0
4	0	0	0	**0.843**	0	0	0	0	**1.186**	0
5	0	0	0	0	**0.830**	0	0	0	0	**1.205**

different from the existing penalties for estimating a sparse precision matrix, is more practical in control chart applications in terms of producing more meaningful estimates of a sparse in-control covariance matrix.

3.2 *ARL performance study and comparison*

In this section we study the ARL performance of the proposed LMEWMC chart and compare it with that of the MaxMEWMV (Yeh *et al.* 2005), MEWMS (Huwang *et al.* 2007) and MEWMC (Hawkins and Maboudou-Tchao 2008) charts. Note that these existing charts are specifically designed to detect changes in the process covariance matrix with individual observations. Most of the other existing charts for monitoring the covariance matrix require that $m > p$ (or at least $m \geq 1$). Nevertheless, despite the fact that these existing charts all belong to EWMA-type control charts, they have never been compared in the literature.

We study and compare the performance of the proposed LMEWMC chart and the three existing charts under four different out-of-control covariance matrices, denoted as $\boldsymbol{\Sigma}_{\mathrm{OC}_i}$, $i = 1, 2, 3$ and 4. The four out-of-control covariance matrices considered are

$$\boldsymbol{\Sigma}_{\mathrm{OC}_1} = \begin{pmatrix} 1 & \delta & \delta & \delta & \delta & & & \\ \delta & 1 & \delta & \delta & \delta & & 0 & \\ \delta & \delta & 1 & \delta & \delta & & & \\ \delta & \delta & \delta & 1 & \delta & & & \\ \delta & \delta & \delta & \delta & 1 & & & \\ & & & & & 1 & & \\ & & 0 & & & & \ddots & \\ & & & & & & & 1 \end{pmatrix}_{p\times p}, \quad \boldsymbol{\Sigma}_{\mathrm{OC}_2} = \begin{pmatrix} 1+\delta & & & & & \\ & 1 & & 0 & & \\ & & 1 & & & \\ & & & 1 & & \\ & 0 & & & \ddots & \\ & & & & & 1 \end{pmatrix}_{p\times p},$$

$$\boldsymbol{\Sigma}_{\mathrm{OC}_3} = \begin{pmatrix} 1 & \delta & & & \\ \delta & 1 & & 0 & \\ & & 1 & & \\ & 0 & & \ddots & \\ & & & & 1 \end{pmatrix}_{p\times p}, \quad \boldsymbol{\Sigma}_{\mathrm{OC}_4} = \begin{pmatrix} 1+\delta^2 & \delta & & & \\ \delta & 1+\delta^2 & & 0 & \\ & & 1 & & \\ & 0 & & \ddots & \\ & & & & 1 \end{pmatrix}_{p\times p}.$$

In $\boldsymbol{\Sigma}_{\mathrm{OC}_1}$, all correlation components of the top left half corner of the covariance matrix change from 0 to δ. In $\boldsymbol{\Sigma}_{\mathrm{OC}_2}$, the only change in the covariance matrix comes from the variance of the first variable, which increases from 1 to $1+\delta$. The change in $\boldsymbol{\Sigma}_{\mathrm{OC}_3}$ stems from increasing the correlation between the first and second variables from 0 to δ. For $\boldsymbol{\Sigma}_{\mathrm{OC}_4}$, the variances of the first and second variables both increase by δ^2, while the correlation between these two variables increases to δ.

Note that $\boldsymbol{\Sigma}_{\mathrm{OC}_2}$, $\boldsymbol{\Sigma}_{\mathrm{OC}_3}$ and $\boldsymbol{\Sigma}_{\mathrm{OC}_4}$ were also considered by Hawkins and Maboudou-Tchao (2008). As noted in their paper, $\boldsymbol{\Sigma}_{\mathrm{OC}_2}$ corresponds to a change of the eigenvalues from $1, 1, \ldots, 1$ to δ^2, $1, \ldots, 1$. Further, $\boldsymbol{\Sigma}_{\mathrm{OC}_3}$ corresponds to a change of the eigenvalues to $1+\delta$, $1-\delta$, $1, \ldots, 1$, while $\boldsymbol{\Sigma}_{\mathrm{OC}_4}$ indicates a change of the eigenvalues to $1+\delta^2+\delta$, $1+\delta^2-\delta$, $1, \ldots, 1$. We considered the cases when $p = 5$, 10, 20, and $\delta = 0.05$ to 0.50. All simulations were carried out using $\omega = 0.1$ to calculate $\mathbf{S}_i$ following Equation (2) and the simulated ARL values were calculated using 10,000 simulations.

In addition to using ARL as a performance measure, Han and Tsung (2006) proposed a relative mean index (RMI) for evaluating the ARL performance of a control chart over a range of change magnitudes in the process parameters. The same index was also used by Zou and Qiu (2009) and Han *et al*. (2010). The RMI is defined as

$$\mathrm{RMI} = \frac{1}{n}\sum_{i=1}^{n}\left[\frac{ARL_{\delta_i} - ARL_{\delta_i,\min}}{ARL_{\delta_i,\min}}\right],$$

where $ARL_{\delta_i,\min}$ is the minimum ARL for detecting a shift magnitude equal to δ_i of the group of control charts to be compared and ARL_{δ_i} is the ARL under δ_i of the control chart for which the RMI is to be calculated. The relative mean index is the sum over all shift magnitudes divided by the total number of shift magnitudes considered. If the RMI of a given control chart is close to 0, it is an indication that the control chart performs relatively better in general than other charts over a range of change magnitudes. The simulation results are summarised in Tables 3–6 for $\boldsymbol{\Sigma}_{\mathrm{OC}_1}$, $\boldsymbol{\Sigma}_{\mathrm{OC}_2}$, $\boldsymbol{\Sigma}_{\mathrm{OC}_3}$ and $\boldsymbol{\Sigma}_{\mathrm{OC}_4}$, respectively.

Table 3 summarises the ARL values of the competing charts under $\boldsymbol{\Sigma}_{\mathrm{OC}_1}$ whose changes from $\boldsymbol{\Sigma}_0$ occur in the upper left half of the matrix. When $p = 5$, the MEWMC and LMEWMC ($\lambda = 0.02$) charts have practically the same best performance, while the MaxMEWMV chart comes in second. The poor performance of the MEWMS chart indicates that the trace of $\mathbf{S}_i$ is not effective in detecting change patterns under $\boldsymbol{\Sigma}_{\mathrm{OC}_1}$. When p increases to 10, the MEWMC and LMEWMC ($\lambda = 0.1$, 0.2) charts still give practically the same best performance. All four charts improve when p increases. If p increases further to 20, the proposed LMEWMC chart with $\lambda = 0.4$ has the best overall performance in terms of having the lowest RMI. It is interesting to point out that when $p = 20$, the MaxMEWMV chart actually has a better overall performance than the MEWMC chart, with the former being better for larger δ values ($\delta \geq 0.25$). The LMEWMC chart also outperforms the MEWMC chart for $0.15 \leq \delta \leq 0.5$. All the charts considered utilise the same EWMA equation in accumulating historical observations by calculating $\mathbf{S}_i$; however, the added penalty gives the LMEWMC chart more flexibility. In general, the LMEWMC chart is quite appealing for detecting $\boldsymbol{\Sigma}_{\mathrm{OC}_1}$. Since the covariance matrix, and by extension the precision matrix, is sparse, the use of a lasso-type penalty forces small estimates of the off-diagonal elements to zero and, thus, makes possible changes in the upper left block more prominent. Such an advantage appears to be more profound when the dimensionality of the quality characteristic becomes larger. The performance of the LMEWMC chart depends on p as well as the tuning parameter λ. Under $\boldsymbol{\Sigma}_{\mathrm{OC}_1}$, we plot in Figure 1(a) the RMI value as a function of the λ value for $p = 5$, 10, 20. The graph indicates that, as far as using the LMEWMC chart to detect the change pattern in $\boldsymbol{\Sigma}_{\mathrm{OC}_1}$ is concerned, setting $\lambda = 0.3$ seems to produce a small RMI value for the various p values considered.

The ARL values for detecting $\boldsymbol{\Sigma}_{\mathrm{OC}_2}$, which has a change only in the variance of the first variable, are summarised in Table 4. When $p = 5$, the proposed LMEWMC ($\lambda = 1.0$) chart has the best overall performance. The MaxMEWMV chart comes in second, while the MEWMS chart comes in third. It is worth pointing out that, as far as detecting $\boldsymbol{\Sigma}_{\mathrm{OC}_2}$ is concerned, the MEWMC chart has the poorest performance among the four competing charts. The same performance pattern holds for $p = 10$ and $p = 20$. Figure 1(b) indicates that, by choosing

Table 3. ARL comparison for $\boldsymbol{\Sigma}_{OC_1}$ ($\omega = 0.1$).

					LMEWMC (λ)										
p	δ	MEWMS	MEWMC	max D_i	0.02	0.04	0.06	0.08	0.1	0.2	0.3	0.4	0.8	1	1.2
5	0.00	200.9	200.3	199.3	199.3	200.4	200.3	200.4	199.8	200.5	200.7	199.8	200.5	200.5	200.8
5	0.05	200.4	196.7	196.8	195.7	196.4	196.7	197.2	198.0	196.6	199.0	197.1	199.2	199.4	200.8
5	0.10	198.6	184.0	191.5	183.5	184.7	184.8	185.6	186.4	185.9	187.7	188.1	195.7	198.6	200.5
5	0.15	194.9	168.0	182.0	167.1	167.4	168.8	169.9	169.8	170.6	172.6	173.4	188.4	196.0	199.7
5	0.20	190.9	148.1	167.1	147.5	147.6	148.0	149.1	150.0	151.0	152.5	156.4	179.2	191.6	198.0
5	0.25	185.9	128.6	152.7	128.3	127.6	128.3	129.1	130.0	131.7	134.1	136.2	166.2	185.0	195.9
5	0.30	181.9	109.2	137.9	109.3	109.4	109.8	110.6	111.5	113.5	115.9	118.2	150.3	176.0	190.8
5	0.35	177.4	91.6	122.5	91.8	92.3	93.2	93.7	94.2	96.1	98.9	101.3	133.6	162.7	184.6
5	0.40	171.7	76.4	107.6	76.6	77.3	77.8	78.3	79.1	81.2	83.3	85.9	117.3	146.9	175.7
5	0.45	165.8	64.7	94.3	64.9	65.3	66.0	66.6	66.9	68.7	71.0	73.0	100.6	131.3	161.3
5	0.50	157.7	54.8	82.9	55.0	55.5	55.9	56.5	56.9	58.6	60.2	61.9	85.5	114.5	145.4
RMI		0.73	0.00	0.24	0.00	0.01	0.01	0.02	0.02	0.04	0.06	0.08	0.32	0.55	0.74
10	0.00	200.2	199.8	200.5	199.8	199.8	199.5	200.6	200.1	199.1	199.8	199.2	200.2	199.7	199.9
10	0.05	197.3	181.2	191.6	181.8	182.0	182.4	182.8	181.7	180.7	183.8	184.7	192.4	196.8	198.5
10	0.10	190.2	144.7	165.8	145.5	144.8	145.0	145.4	144.9	145.4	147.3	149.4	172.4	186.0	194.9
10	0.15	177.4	107.6	130.4	108.1	107.3	107.6	108.0	107.7	107.8	109.5	111.8	146.4	171.0	189.6
10	0.20	163.2	78.4	98.3	78.5	78.6	78.5	79.0	78.7	79.1	80.5	82.9	119.2	151.7	180.3
10	0.25	147.8	59.5	72.5	59.4	59.5	59.5	59.6	59.6	59.8	60.4	62.4	95.9	130.5	165.9
10	0.30	132.1	46.7	55.4	46.6	46.3	46.5	46.6	46.5	46.6	47.3	48.5	76.7	108.9	148.7
10	0.35	117.7	38.3	43.6	38.0	37.8	37.6	37.5	37.5	37.6	37.9	39.0	62.8	90.6	130.4
10	0.40	104.4	32.0	35.5	31.8	31.7	31.6	31.6	31.5	31.4	31.5	32.4	51.9	75.9	112.0
10	0.45	92.7	27.6	29.9	27.3	27.2	27.1	27.0	26.9	26.7	26.8	27.5	43.6	64.3	95.2
10	0.50	81.6	24.3	25.7	24.1	23.9	23.7	23.6	23.4	23.2	23.4	24.0	37.5	55.1	81.5
RMI		1.49	0.01	0.16	0.01	0.01	0.01	0.01	0.00	0.00	0.01	0.04	0.50	1.01	1.66
20	0.00	200.8	200.1	200.4	199.1	200.0	200.5	199.8	199.3	200.7	199.1	199.6	200.9	200.5	199.9
20	0.05	195.5	167.5	184.4	169.0	170.0	171.4	172.6	172.2	172.2	173.7	174.2	184.8	191.3	195.5
20	0.10	177.4	118.6	140.6	117.2	119.0	119.7	120.3	120.2	121.6	121.8	120.2	147.7	167.9	186.5
20	0.15	153.2	80.6	91.6	79.0	79.1	79.4	80.1	80.1	79.8	78.0	77.3	107.7	138.0	169.0
20	0.20	130.2	59.5	61.5	57.8	57.6	57.6	57.8	57.7	57.0	55.1	54.4	77.4	108.8	149.0
20	0.25	107.5	46.9	43.7	45.3	44.9	44.7	44.8	44.5	42.9	41.2	40.2	59.0	84.4	125.1
20	0.30	88.7	39.0	33.3	37.4	36.8	36.5	36.3	36.1	34.6	32.8	31.9	46.6	67.8	103.0
20	0.35	73.2	33.9	26.8	32.3	31.7	31.3	31.0	30.7	28.9	27.3	26.5	38.0	56.1	85.3
20	0.40	61.4	30.2	22.5	28.6	27.9	27.4	27.0	26.7	25.0	23.5	22.8	32.1	47.2	71.4
20	0.45	52.1	27.3	19.4	25.9	25.1	24.6	24.3	23.9	22.1	20.7	20.0	28.0	40.2	61.4
20	0.50	44.2	25.2	17.1	23.8	22.9	22.3	21.9	21.5	19.8	18.6	18.0	25.0	35.5	53.3
RMI		1.33	0.20	0.08	0.16	0.14	0.14	0.13	0.12	0.08	0.04	0.02	0.39	0.89	1.67

$\lambda = 1.2$, the LMEWMC chart has the best overall RMI performance in detecting $\boldsymbol{\Sigma}_{OC_2}$ for the various p values considered.

Table 5 summarises the comparison results under $\boldsymbol{\Sigma}_{OC_3}$, which has changes occurring only in the correlation between the first and second variables. The MEWMC chart has the best overall performance, although the LMEWMC chart has practically the same overall performance in terms of the RMI value. The MaxMEWMV chart comes in second, while the MEWMS chart has the poorest overall performance. Figure 1(c) suggests that setting $\lambda = 0.02$ when constructing the LMEWMC chart will produce small overall RMI values for the dimensionalities considered. For detecting $\boldsymbol{\Sigma}_{OC_4}$, which has changes in the variance of the first variable and the correlation between the first and second variables, the simulation results are summarised in Table 6. The results suggest that the proposed LMEWMC chart has the best overall performance among the four competing charts. The MaxMEWMV chart has slightly better overall performance than the MEWMC chart in terms of the RMI value for $p = 10$ and 20. The MEWMS chart, on the other hand, is relatively ineffective in detecting $\boldsymbol{\Sigma}_{OC_4}$. Figure 1(d) suggests that, as far as detecting the change pattern in $\boldsymbol{\Sigma}_{OC_4}$ is concerned, the LMEWMC chart with $\lambda = 0.4$ gives the best overall performance for the p values considered.

Table 4. ARL comparison for $\mathbf{\Sigma}_{OC_2}$ ($\omega = 0.1$).

					LMEWMC (λ)										
p	δ	MEWMS	MEWMC	max D_i	0.02	0.04	0.06	0.08	0.1	0.2	0.3	0.4	0.8	1	1.2
5	0.00	200.9	200.3	199.3	199.3	200.4	200.3	200.4	199.8	200.5	200.7	199.8	200.5	200.5	200.8
5	0.05	181.4	189.9	181.3	188.6	187.3	186.4	186.7	186.1	184.1	182.6	182.6	181.8	181.5	183.0
5	0.10	163.1	177.8	161.0	176.3	174.0	173.0	172.2	171.7	167.5	165.5	163.6	161.8	161.3	162.8
5	0.15	145.9	163.1	142.0	161.7	160.1	158.7	157.7	156.8	151.3	148.8	146.8	142.3	142.0	143.1
5	0.20	130.5	150.0	124.9	148.4	146.5	144.4	143.1	141.7	136.3	134.0	131.4	123.7	123.4	124.5
5	0.25	115.9	137.2	109.3	135.8	133.6	131.3	129.4	128.1	123.4	120.0	116.5	107.0	107.4	108.2
5	0.30	104.7	124.9	95.9	123.6	121.0	119.4	117.0	115.7	109.6	106.6	104.0	93.9	93.0	93.9
5	0.35	94.7	113.0	84.7	111.4	109.3	107.1	105.7	103.9	98.0	95.3	92.7	81.7	81.0	81.4
5	0.40	85.8	102.5	74.4	100.6	98.1	96.3	94.9	93.6	88.2	85.6	82.7	71.7	70.8	71.2
5	0.45	77.9	92.4	66.0	91.2	89.0	87.0	85.4	84.1	79.3	77.3	73.9	63.4	62.3	62.3
5	0.50	70.7	83.9	59.2	82.5	80.3	78.2	76.8	75.9	72.0	69.6	66.5	56.3	55.3	55.4
RMI		0.12	0.30	0.03	0.28	0.26	0.24	0.22	0.21	0.16	0.13	0.10	0.01	0.00	0.01
10	0.00	200.2	199.8	200.5	199.8	199.8	199.5	200.6	200.1	199.1	199.8	199.2	200.2	199.7	199.9
10	0.05	190.0	195.5	186.5	193.8	193.0	192.3	192.3	190.3	186.7	187.4	188.0	187.5	188.0	187.1
10	0.10	179.4	188.1	172.6	187.0	185.0	183.4	182.9	179.9	175.4	175.7	174.9	173.0	173.1	172.5
10	0.15	168.9	181.2	157.0	178.7	176.3	173.8	171.8	169.0	164.3	164.0	162.4	158.4	158.2	157.9
10	0.20	156.3	172.9	142.6	170.1	166.7	163.4	161.4	159.2	153.1	152.8	151.3	144.2	143.8	143.4
10	0.25	146.0	164.3	128.2	160.9	157.4	153.6	151.7	149.1	143.2	141.8	140.4	131.1	128.6	128.2
10	0.30	136.5	154.5	115.1	151.3	147.6	144.2	142.2	139.4	133.9	132.0	129.9	117.5	114.1	112.7
10	0.35	126.1	145.7	103.3	142.6	138.5	135.0	133.0	130.1	124.8	122.5	119.8	104.9	100.1	99.0
10	0.40	116.6	137.8	91.9	133.7	129.7	126.4	124.8	121.7	115.7	113.8	110.4	93.1	88.5	87.4
10	0.45	108.7	129.1	82.2	125.5	121.3	118.0	115.8	112.7	107.2	105.6	101.9	83.3	78.3	77.4
10	0.50	100.8	121.7	73.3	117.4	113.5	109.9	107.3	105.2	100.0	97.5	93.4	74.6	69.9	69.0
RMI		0.21	0.36	0.02	0.33	0.30	0.28	0.26	0.23	0.19	0.17	0.15	0.04	0.01	0.00
20	0.00	200.8	200.1	200.4	199.1	200.0	200.5	199.8	199.3	200.7	199.1	199.6	200.9	200.5	199.9
20	0.05	194.4	197.4	190.5	195.3	195.1	194.5	193.7	192.7	191.9	191.0	191.2	192.9	192.9	192.5
20	0.10	188.2	194.5	180.7	191.3	190.4	188.7	188.1	186.3	184.0	183.4	182.6	184.6	184.3	183.7
20	0.15	182.5	190.9	168.7	186.2	185.2	183.0	181.3	180.1	176.5	175.6	174.3	174.6	173.5	172.7
20	0.20	175.3	186.7	157.7	181.9	179.7	176.1	175.2	173.6	168.5	167.2	165.2	163.7	161.3	159.7
20	0.25	168.3	181.9	145.8	175.7	173.0	168.8	168.1	165.9	160.3	159.2	156.8	152.7	148.7	146.8
20	0.30	160.8	177.0	133.8	169.4	165.4	162.2	160.9	158.4	153.9	152.1	149.4	141.3	136.2	133.4
20	0.35	154.3	171.4	121.7	163.6	159.2	155.9	153.7	151.4	146.9	145.1	141.6	130.8	124.0	120.3
20	0.40	147.0	166.3	109.2	157.3	152.6	149.5	147.0	144.7	140.9	138.7	134.3	119.7	112.0	107.1
20	0.45	139.9	160.4	99.5	151.2	146.6	143.5	140.8	138.8	134.8	132.0	127.4	108.8	101.3	95.3
20	0.50	132.8	154.8	89.8	145.3	141.0	137.2	134.8	133.0	128.9	126.0	120.6	99.4	90.2	84.9
RMI		0.23	0.35	0.01	0.29	0.27	0.25	0.23	0.22	0.19	0.17	0.15	0.07	0.03	0.01

As mentioned above, the three existing charts for detecting changes in the process covariance matrix with individual observations, the MaxMEWMV, MEWMS and MEWMC charts, have never been compared in the existing literature. Therefore, our comparison also sheds some light on how these existing methods match up with one another. The results indicate that none of the existing charts is necessarily the best performing chart, and could even be the worst performer for certain out-of-control covariance matrices. On the other hand, the proposed LMEWMC chart, which is based on a lasso-type penalised likelihood estimation, is either the best performing chart among the four competing charts ($\mathbf{\Sigma}_{OC_2}$ and $\mathbf{\Sigma}_{OC_4}$), or is practically equivalent to the best performer among the existing charts ($\mathbf{\Sigma}_{OC_1}$ and $\mathbf{\Sigma}_{OC_3}$).

3.3 *Optimal choice of λ*

It is evident from the above study that the optimal choice of λ varies with the target shift patterns. We have highlighted suggested choices for λ for the shift patterns studied in the preceding section. A fixed λ may not work

Table 5. ARL comparison for $\boldsymbol{\Sigma}_{OC_3}$ ($\omega = 0.1$).

					LMEWMC (λ)										
p	δ	MEWMS	MEWMC	max D_i	0.02	0.04	0.06	0.08	0.1	0.2	0.3	0.4	0.8	1	1.2
5	0.00	200.9	200.3	199.3	199.3	200.4	200.3	200.4	199.8	200.5	200.7	199.8	200.5	200.5	200.8
5	0.05	200.4	196.7	196.8	195.7	196.4	196.7	197.2	198.0	196.6	199.0	197.1	199.2	199.4	200.8
5	0.10	198.6	184.0	191.5	183.5	184.7	184.8	185.6	186.4	185.9	187.7	188.1	195.7	198.6	200.5
5	0.15	194.9	168.0	182.0	167.1	167.4	168.8	169.9	169.8	170.6	172.6	173.4	188.4	196.0	199.7
5	0.20	190.9	148.1	167.1	147.5	147.6	148.0	149.1	150.0	151.0	152.5	156.4	179.2	191.6	198.0
5	0.25	185.9	128.6	152.7	128.3	127.6	128.3	129.1	130.0	131.7	134.1	136.2	166.2	185.0	195.9
5	0.30	181.9	109.2	137.9	109.3	109.4	109.8	110.6	111.5	113.5	115.9	118.2	150.3	176.0	190.8
5	0.35	177.4	91.6	122.5	91.8	92.3	93.2	93.7	94.2	96.1	98.9	101.3	133.6	162.7	184.6
5	0.40	171.7	76.4	107.6	76.6	77.3	77.8	78.3	79.1	81.2	83.3	85.9	117.3	146.9	175.7
5	0.45	165.8	64.7	94.3	64.9	65.3	66.0	66.6	66.9	68.7	71.0	73.0	100.6	131.3	161.3
5	0.50	157.7	54.8	82.9	55.0	55.5	55.9	56.5	56.9	58.6	60.2	61.9	85.5	114.5	145.4
RMI		0.73	0.00	0.24	0.00	0.01	0.01	0.02	0.02	0.04	0.06	0.08	0.32	0.55	0.74
10	0.00	200.2	199.8	200.5	199.8	199.8	199.5	200.6	200.1	199.1	199.8	199.2	200.2	199.7	199.9
10	0.05	200.3	198.0	200.2	197.6	198.1	198.7	199.4	198.5	197.3	198.3	198.4	199.1	199.3	200.1
10	0.10	199.5	192.1	197.3	192.6	192.5	192.7	194.5	193.5	192.5	194.3	194.7	196.2	198.0	199.7
10	0.15	197.8	182.2	193.9	183.6	183.8	184.2	185.4	184.9	183.8	187.7	188.6	192.5	196.5	199.4
10	0.20	195.9	171.6	188.1	171.8	172.0	172.8	174.1	173.8	172.6	177.6	178.3	185.9	192.3	198.0
10	0.25	194.5	158.4	182.4	159.3	159.0	159.3	160.7	159.7	160.5	164.8	166.3	176.4	186.1	196.0
10	0.30	192.4	142.8	174.3	144.2	145.1	145.8	146.6	146.3	147.3	151.1	153.0	165.5	178.7	191.7
10	0.35	189.8	128.6	165.8	129.4	131.0	131.5	132.2	131.9	132.9	137.0	137.9	152.3	167.9	186.0
10	0.40	186.0	113.5	156.3	114.2	115.9	116.7	117.9	118.0	119.0	122.3	122.8	136.5	155.1	177.2
10	0.45	182.6	99.8	147.1	101.1	102.3	103.2	104.4	104.6	106.2	107.9	107.8	120.7	140.3	165.9
10	0.50	177.6	86.8	136.4	88.0	89.0	89.8	91.2	91.7	93.1	95.2	94.9	105.8	125.1	152.0
RMI		0.38	0.00	0.23	0.01	0.01	0.02	0.03	0.02	0.03	0.05	0.05	0.13	0.22	0.33
20	0.00	200.8	200.1	200.4	199.1	200.0	200.5	199.8	199.3	200.7	199.1	199.6	200.9	200.5	199.9
20	0.05	200.4	199.0	199.8	197.7	199.1	199.8	199.8	198.3	199.1	198.0	199.5	200.5	200.5	199.5
20	0.10	200.9	196.2	198.5	195.2	197.4	197.4	197.6	196.3	196.8	196.7	197.3	199.6	199.5	199.5
20	0.15	201.1	191.5	197.4	191.5	193.0	193.1	193.6	192.8	193.4	194.2	194.2	197.6	198.2	198.8
20	0.20	199.9	184.9	195.2	185.5	187.5	188.7	188.3	188.2	188.4	190.3	190.9	194.3	196.0	197.7
20	0.25	198.2	178.1	193.0	179.2	181.3	181.6	182.4	181.6	183.2	184.3	184.3	189.7	192.0	195.6
20	0.30	196.2	169.0	190.1	170.8	172.8	173.5	174.6	174.2	176.0	177.1	177.6	183.6	186.8	192.5
20	0.35	194.5	159.7	186.1	161.5	163.2	164.1	165.8	165.1	167.6	168.4	167.8	173.5	178.5	188.1
20	0.40	191.8	149.7	182.0	152.2	153.0	154.1	155.9	156.2	157.8	158.7	157.8	161.5	167.9	180.9
20	0.45	189.3	139.1	177.5	140.9	142.3	143.8	145.8	145.6	147.6	148.6	147.4	148.1	155.3	171.3
20	0.50	186.6	127.8	172.2	129.6	131.6	133.0	134.7	134.7	137.9	137.7	136.6	134.3	142.0	159.9
RMI		0.18	0.00	0.13	0.01	0.02	0.02	0.03	0.03	0.04	0.04	0.04	0.06	0.08	0.12

well for all shift patterns. Therefore, the choice of the tuning parameter λ should be made with certain engineering knowledge. Failure pattern analysis based on historical data is usually helpful in identifying potential shift patterns.

Although only a limited number of shift patterns are studied in this work, the proposed chart itself is not limited to detecting these shifts. It is expected that the proposed chart should work well for cases whose shift patterns could be better captured by the penalised algorithm. In such cases, the choice of λ could be made based on some data-driven method. Zou *et al.* (2011) proposed an extended Bayesian criterion (EBIC) to guide the choice of tuning parameter and diagnostics. Lian (2011) suggested a BIC-type criterion for choosing the tuning parameter in penalised covariance matrix estimation. Lian (2011) showed that his BIC is capable of consistently detecting the sparsity pattern in Ω. One can similarly adapt his criterion, choosing λ that minimises EBIC or BIC.

4. A real example

In this section, we apply the proposed LMEWMC chart to a real example and compare its performance with that of the MaxMEWMV, MEWMS and MEWMC charts.

Table 6. ARL comparison for $\mathbf{\Sigma}_{OC_4}$ ($\omega = 0.1$).

					LMEWMC (λ)										
p	δ	MEWMS	MEWMC	max D_i	0.02	0.04	0.06	0.08	0.1	0.2	0.3	0.4	0.8	1	1.2
5	0.00	200.9	200.3	199.3	199.3	200.4	200.3	200.4	199.8	200.5	200.7	199.8	200.5	200.5	200.8
5	0.05	198.2	196.1	195.2	195.2	195.5	195.9	196.0	196.5	195.1	196.7	195.6	197.4	197.5	199.1
5	0.10	190.2	181.8	184.7	181.5	181.8	181.9	182.4	182.5	180.9	182.4	181.9	188.3	191.0	193.5
5	0.15	178.5	162.2	166.7	161.6	161.1	161.1	161.5	160.8	159.3	159.7	161.2	173.2	180.6	184.7
5	0.20	164.4	140.8	145.6	140.0	139.1	138.3	137.9	137.4	135.8	135.9	137.0	154.4	164.8	172.3
5	0.25	146.8	120.0	125.3	119.3	118.6	117.0	116.8	116.4	114.4	114.0	114.2	133.3	146.9	155.0
5	0.30	127.8	101.3	105.6	100.3	98.9	98.4	97.9	97.1	94.5	93.6	93.9	111.4	127.3	137.4
5	0.35	110.6	84.9	87.6	83.8	82.7	81.5	80.7	80.3	77.7	76.9	76.6	92.4	107.1	118.3
5	0.40	94.5	71.3	72.9	70.6	69.4	68.4	67.6	67.1	64.8	63.9	63.2	75.1	89.0	99.1
5	0.45	79.5	60.7	61.2	60.1	59.2	58.4	57.8	57.1	54.6	53.5	52.3	61.7	73.2	82.8
5	0.50	66.5	52.2	50.8	51.5	50.5	49.7	49.2	48.5	46.2	44.8	43.8	50.8	60.5	68.1
RMI		0.30	0.08	0.10	0.07	0.06	0.05	0.05	0.04	0.02	0.01	0.00	0.14	0.27	0.36
10	0.00	200.2	199.8	200.5	199.8	199.8	199.5	200.6	200.1	199.1	199.8	199.2	200.2	199.7	199.9
10	0.05	199.3	197.8	199.0	197.3	197.5	198.1	198.6	197.9	195.8	197.4	197.3	197.8	198.2	198.5
10	0.10	195.7	190.1	192.9	190.7	190.1	189.5	191.6	189.8	187.5	189.6	189.7	191.9	193.8	195.4
10	0.15	189.3	179.5	183.8	179.5	178.7	178.7	178.6	178.0	175.1	177.6	177.7	182.3	186.4	188.8
10	0.20	181.0	167.1	170.7	166.3	165.4	164.1	164.1	162.1	158.9	160.8	161.5	168.6	174.3	180.0
10	0.25	169.4	152.6	154.4	151.8	149.8	148.7	147.2	146.0	143.1	143.3	144.5	151.6	160.5	167.3
10	0.30	155.2	137.4	138.7	135.9	133.9	132.2	131.2	129.5	126.2	126.3	125.9	131.9	143.2	152.7
10	0.35	140.9	122.0	121.6	120.7	118.7	116.3	115.5	113.5	109.8	109.0	107.8	111.2	124.3	135.1
10	0.40	126.7	108.4	105.0	106.5	103.9	102.1	100.9	99.2	95.5	94.5	91.9	93.6	104.4	117.7
10	0.45	112.0	94.8	88.8	92.9	90.7	88.5	87.5	85.8	82.5	80.6	77.4	77.1	87.0	98.6
10	0.50	96.9	83.5	75.3	81.6	79.3	77.3	76.1	74.8	71.1	69.2	66.5	64.2	72.5	82.4
RMI		0.23	0.11	0.09	0.10	0.08	0.07	0.06	0.05	0.02	0.02	0.01	0.03	0.10	0.17
20	0.00	200.8	200.1	200.4	199.1	200.0	200.5	199.8	199.3	200.7	199.1	199.6	200.9	200.5	199.9
20	0.05	200.1	198.8	198.7	197.6	198.7	199.1	199.0	197.8	198.3	197.6	198.5	199.7	199.8	199.0
20	0.10	198.4	195.2	194.8	194.1	195.6	195.2	194.9	193.7	194.0	193.7	194.1	196.7	196.9	196.5
20	0.15	194.8	189.8	190.2	189.0	189.7	188.9	189.2	187.0	186.7	187.5	186.4	190.9	192.4	192.8
20	0.20	189.3	183.3	182.5	181.1	182.0	180.4	180.5	179.1	177.6	178.6	177.1	182.8	184.6	186.9
20	0.25	182.8	175.3	171.4	171.8	172.2	170.5	170.0	168.0	166.3	166.0	165.1	169.0	173.2	178.4
20	0.30	175.4	165.5	159.8	161.8	160.9	158.9	158.0	156.2	154.2	153.7	151.7	154.4	158.8	166.5
20	0.35	165.2	156.9	147.1	151.7	148.7	146.7	146.5	144.5	141.9	140.2	138.1	136.8	141.8	152.0
20	0.40	153.5	146.6	132.8	141.1	137.1	135.2	134.3	133.0	129.5	128.0	124.6	119.5	123.4	134.0
20	0.45	141.6	136.7	116.9	129.7	126.3	124.0	123.1	120.7	117.7	115.2	111.1	101.4	104.3	115.0
20	0.50	128.7	127.0	101.1	119.5	115.3	112.9	110.8	108.5	105.4	102.8	98.4	85.0	87.6	97.5
RMI		0.18	0.14	0.07	0.11	0.10	0.09	0.08	0.07	0.06	0.05	0.03	0.01	0.03	0.08

Hawkins and Maboudou-Tchao (2008) presented a real data set from an ambulatory monitoring application. Four physiological variables, mean systolic blood pressure (SBP), mean diastolic blood pressure (DBP), mean of heart rate (HR) and overall mean arterial pressure (MAP), were summarised and reported each week. Hawkins and Maboudou-Tchao (2008) obtained estimates of the in-control mean and covariance matrix, and transformed a data set having 24 observations into 24 independent observations each generated from a four-dimensional normal distribution with zero mean and identity covariance matrix. The transformation was done based on the regression adjustment method of Hawkins (1993). The four transformed variables are denoted U_1, U_2, U_3 and U_4, respectively. Specifically, U_1 is the standardised SBP, U_2 is the residual, scaled to unit standard deviation, of the regression of DBP on SBP, U_3 is the residual of the regression of HR on SBP and DBP, standardised to unit standard deviation, and U_4 is the standardised residual of the regression of MAP on SBP, DBP and HR. For a more detailed account of the data set, see Hawkins and Maboudou-Tchao (2008).

Following the treatment of Hawkins and Maboudou-Tchao (2008), here we monitor the transformed variables U_1, U_2, U_3 and U_4. Similar to the settings of Hawkins and Maboudou-Tchao (2008), the four competing charts studied in the previous sections are all set up to monitor the 24 individual observations such that the in-control ARL value of each chart is approximately equal to 500. The resulting control charts are shown in Figure 2. As can be seen

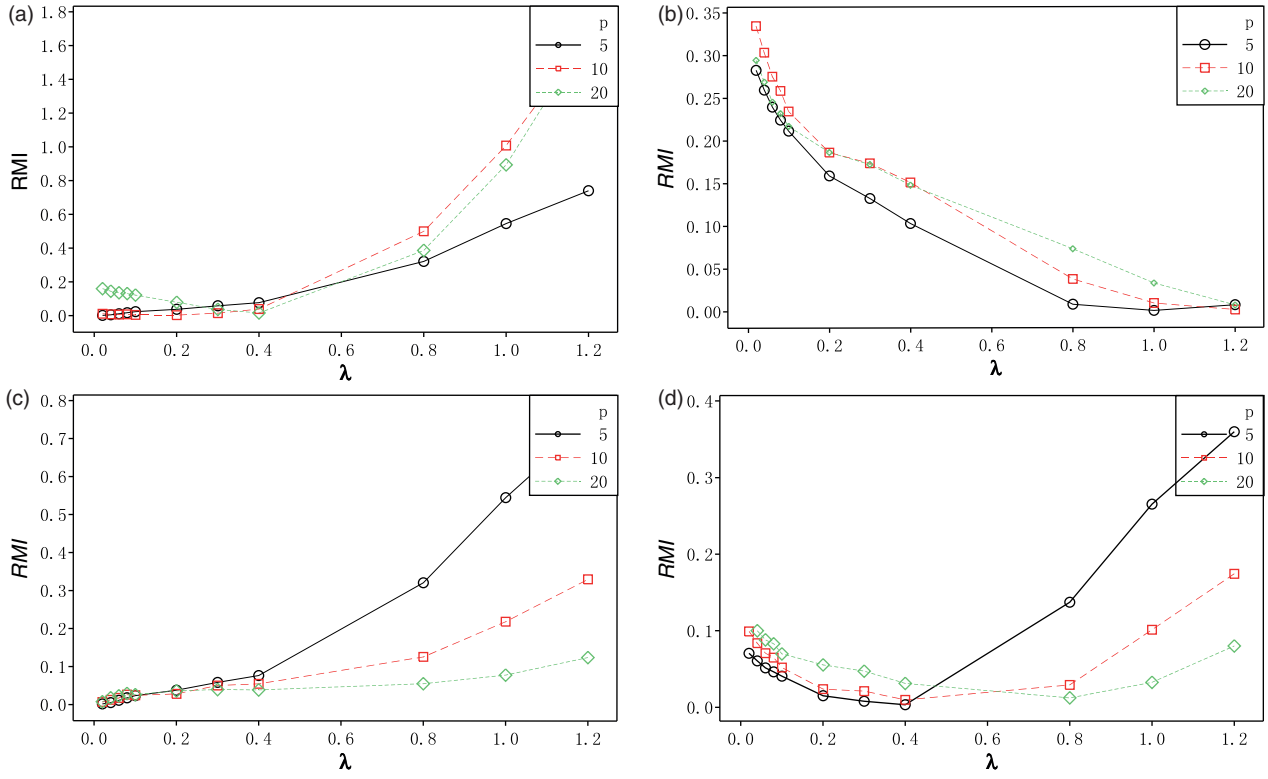

Figure 1. RMI curves under different λ and *p*.

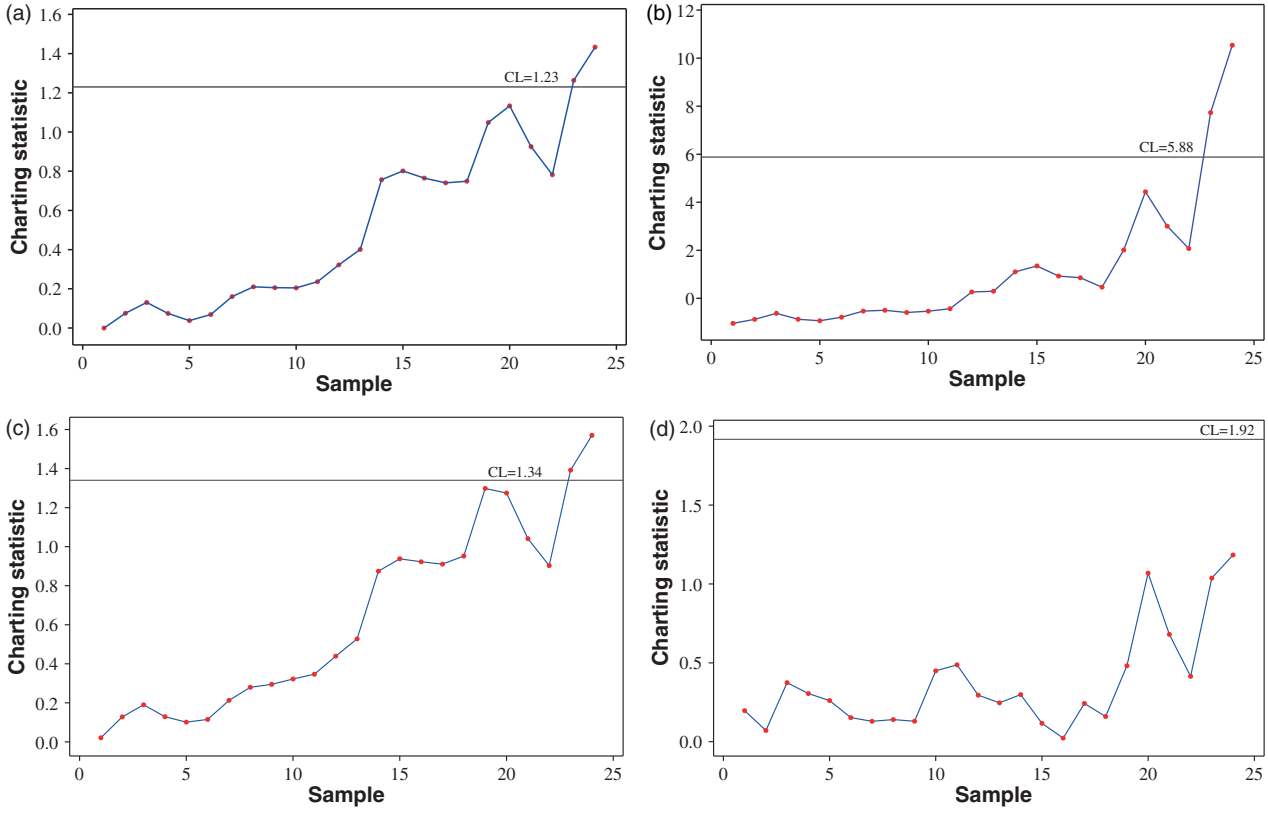

Figure 2. Various control charts for the ambulatory monitoring example.

from the figure, except for the MEWMS chart, all the other charts trigger an out-of-control signal at sample 23. The MEWMS chart does not even produce an out-of-control signal, leading one to further question its effectiveness in detecting an out-of-control covariance matrix in this particular instance. The trend observed for the LMEWMC chart is similar to the MEWMC chart. This is consistent with our analysis in the previous section that, for certain out-of-control covariance matrices, the MEWMC and LMEWMC charts have practically the same performance. This example also demonstrates that the proposed LMEWMC chart can be implemented in practice in very much the same way as a conventional control chart. Hawkins and Maboudou-Tchao (2008) estimated that process changes were introduced into the process starting from observation 6; the authors then conducted an out-of-control analysis based on observations 6–23. For comparison, we also conducted an out-of-control analysis based on the suspected out-of-control observations 6–23.

We first derive the sample covariance matrix, $\mathbf{S}_{23}$, following Equation (2), using observations 6–23. The initial value of the EWMA equation is set to $\mathbf{U}_6\mathbf{U}_6^T$ rather than $\mathbf{I}_4$, as suggested by Huwang *et al*. (2007). Then, a sparse estimate of the precision matrix $\mathbf{\Omega}_{23}$ is calculated using Equation (5),

$$\mathbf{\Omega}_{23} = \begin{pmatrix} 1.543 & -0.016 & 0 & -0.258 \\ -0.016 & 0.922 & -0.089 & 0.098 \\ 0 & -0.089 & 1.716 & 0.071 \\ -0.258 & 0.098 & 0.071 & 0.440 \end{pmatrix}.$$

Further, the inverse of $\mathbf{\Omega}_{23}$ gives an estimate of the covariance matrix,

$$\mathbf{\Omega}_{23}^{-1} = \begin{pmatrix} 0.720 & -0.036 & -0.020 & 0.433 \\ -0.036 & 1.129 & 0.070 & -0.281 \\ -0.020 & 0.070 & 0.591 & -0.122 \\ 0.433 & -0.281 & -0.122 & 2.606 \end{pmatrix}.$$

Based on fitting the regressions of each U_j on $U_1, U_2, \ldots, U_{j-1}, j = 2, 3$ and 4, Hawkins and Maboudou-Tchao (2008) concluded that HR, corrected for SBP and DBP, becomes less variable, while MAP, corrected for SBP, DBP and HR, becomes more variable.

From $\mathbf{\Omega}_{23}^{-1}$ we obtained the same conclusions as Hawkins and Maboudou-Tchao (2008), since the variance estimates of U_3 and U_4 are 0.591 and 2.606, respectively. Further, we also observed that the SBP seemed to become less variable. The correlation between U_1 and U_4 also seemed to increase, while the pairs of variables U_1 and U_2, U_1 and U_3, and U_2 and U_3 seem to remain uncorrelated.

5. Conclusions

This paper proposes a lasso-based multivariate exponentially weighted moving covariance chart, the LMEWMC chart, for monitoring the changes in process variability with individual observations. Similar to the existing MEWMS and MEWMC charts, historical observations are first accumulated via an EWMA calculation. Different from the existing charts in which the process covariance matrix is estimated by the sample covariance matrix based on the EWMA of the individual observations, a lasso-type penalty is added to the likelihood estimation of the process precision matrix, which has the effect of forcing the estimates to shrink towards their respective in-control values.

Simulation studies indicated that the proposed LMEWMC chart either has the best performance or performs as good as the best performing existing chart for the types of out-of-control covariance matrices considered in the current paper as well as by Hawkins and Maboudou-Tchao (2008). In addition, the LMEWMC chart is flexible in that the tuning parameter λ can be chosen to obtain different estimates of the process precision matrix. Some guidelines are also provided for how to choose the tuning parameter λ for different types of $\mathbf{\Sigma}_{OC}$. If certain engineering knowledge concerning process failure patterns is available, one can choose λ that produces the best performance under potential failure patterns.

In recent work, Wang and Jiang (2009) proposed a multivariate control chart for monitoring the process mean vector under the assumption that when the mean shifts only a small number of components will actually shift. They also suggested a lasso-type estimate of the process mean vector. In many practical multivariate quality control applications, one typically encounters scenarios in which an out-of-control process is a result of either a shift in the

process mean or a change in the process covariance matrix, or both. Therefore, simultaneous monitoring of the mean vector and the covariance matrix is important from a practical standpoint. In another recent paper, Camci *et al*. (2008) proposed a support vector machines based control chart which can be considered as a non-parametric control chart capable of simultaneously monitoring changes in the process mean and the covariance matrix on a single chart. It would be worthwhile studying how the lasso-type penalised likelihood estimation can be incorporated into simultaneously estimating the mean vector and the covariance matrix, the resulting estimates of which can then be used to construct control charts for simultaneously monitoring the process mean vector and covariance matrix with individual observations. Further, it would also be interesting to investigate how the performance of the lasso-type control charts matches up with that of the support vector machines based control charts. This will be further explored in a follow-up study.

Acknowledgements

We thank the editor and a referee for their comments and suggestions that improved the presentation of the paper. Dr. Bo Li's work is supported, in part, by the National Natural Science Foundation of China (NSFC) (grants 10801086, 70831003 and 71072012). Dr. Kaibo Wang's work is supported by the NSFC under grant 71072012.

References

Alfaro, E., *et al*., 2009. A boosting approach for understanding out-of-control signals in multivariate control charts. *International Journal of Production Research*, 47 (24), 6821–6834.

Alt, F., 1984. Multivariate quality control. *In*: S. Kotz, N.L. Johnson and C.R. Read, eds. *The encyclopedia of statistical sciences*. New York: Wiley, 110–122.

Camci, F., Chin, R.B., and Ellis, R.D., 2008. Robust kernel distance multivariate control chart using support vector principles. *International Journal of Production Research*, 46 (18), 5075–5095.

D'Aspremont, A., Banerjee, O., and El Ghaoui, L., 2008. First-order methods for sparse covariance selection. *Siam Journal on Matrix Analysis and Applications*, 30 (1), 56–66.

Friedman, J., Hastie, T., and Tibshirani, R., 2008. Sparse inverse covariance estimation with the graphical lasso. *Biostatistics*, 9 (3), 432–441.

Gonzalez, I. and Sanchez, I., 2008. Principal alarms in multivariate statistical process control using independent component analysis. *International Journal of Production Research*, 46 (22), 6345–6366.

Han, D. and Tsung, F., 2006. A reference-free Cuscore chart for dynamic mean change detection and a unified framework for charting performance comparison. *Journal of the American Statistical Association*, 101 (473), 368–386.

Han, D., *et al*., 2010. A nonlinear filter control chart for detecting dynamic changes. *Statistica Sinica*, 20, 1077–1096.

Hawkins, D.M., 1993. Regression adjustment for variables in multivariate quality control. *Journal of Quality Technology*, 25 (3), 170–182.

Hawkins, D.M. and Maboudou-Tchao, E.M., 2008. Multivariate exponentially weighted moving covariance matrix. *Technometrics*, 50 (2), 155–166.

Huang, J.Z., *et al*., 2006. Covariance matrix selection and estimation via penalised normal likelihood. *Biometrika*, 93 (1), 85–98.

Huwang, L., Yeh, A.B., and Wu, C.-W., 2007. Monitoring multivariate process variability with individual observations. *Journal of Quality Technology*, 39 (3), 258–278.

Hwarng, H.B., 2008. Toward identifying the source of mean shifts in multivariate SPC: a neural network approach. *International Journal of Production Research*, 46 (20), 5531–5559.

Hwarng, H.B. and Wang, Y., 2010. Shift detection and source identification in multivariate autocorrelated processes. *International Journal of Production Research*, 48 (3), 835–859.

Li, B., Wang, K., and Yeh, A.B., 2012. Monitoring covariance matrix via penalized likelihood estimation. *IIE Transactions*, in press.

Lian, H., 2011. Shrinkage tuning parameter selection in precision matrices estimation. *Journal of Statistical Planning and Inference*, 141 (8), 2839–2848.

Lowry, C.A., *et al*., 1992. A multivariate exponentially weighted moving average control chart. *Technometrics*, 34 (1), 46–53.

Montgomery, D.C. and Wadsworth, H.M., 1972. Some techniques for multivariate quality control applications. *Transactions of the ASQC*. the ASQC, Washington.

Niaki, S.T.A. and Davoodi, M., 2009. Designing a multivariate-multistage quality control system using artificial neural networks. *International Journal of Production Research*, 47 (1), 251–271.

Rothman, A.J., *et al*., 2008. Sparse permutation invariant covariance estimation. *Electronic Journal of Statistics*, 2, 494–515.

Shi, J., 2006. *Stream of variation modeling and analysis for multistage manufacturing processes*. Boca Raton, FL: CRC Press.

Wang, K. and Jiang, W., 2009. High-dimensional process monitoring and fault isolation via variable selection. *Journal of Quality Technology*, 41 (3), 247–258.

Yeh, A.B., Huwang, L., and Wu, C.W., 2005. A multivariate EWMA control chart for monitoring process variability with individual observations. *IIE Transactions on Quality and Reliability Engineering*, 37 (11), 1023–1035.

Zhang, G. and Chang, S.-I., 2008. Multivariate EWMA control charts using individual observations for process mean and variance monitoring and diagnosis. *International Journal of Production Research*, 46 (24), 6855–6881.

Zou, C., Jiang, W., and Tsung, F., 2011. A LASSO-based diagnostic framework for multivariate statistical process control. *Technometrics*, 53 (3), 297–309.

Zou, C. and Qiu, P., 2009. Multivariate statistical process control using LASSO. *Journal of the American Statistical Association*, 104 (488), 1586–1596.